



## Synthesis and photoactivity of a Pt(II) complex based on an *o*-nitrobenzyl-derived ligand

Di Liu, Jialiu Ma, Wen Zhou, Weijiang He\*, Zijian Guo\*

State Key Laboratory of Coordination Chemistry, School of Chemistry and Chemical Engineering, Nanjing University, Nanjing 210093, China

### ARTICLE INFO

#### Article history:

Available online 20 July 2012

Metals in Medicine Special Issue

#### Keywords:

Platinum complex  
Photoactivation  
Cytotoxicity  
Tumor  
DNA

### ABSTRACT

Development of photoactivatable platinum complexes was an attractive approach to improve the anti-cancer behavior of Pt-based agents. In this work, a new photolabile Pt(II) complex, **NMPt**, was prepared using a photosensitive compound, 2-hydroxy-2-(2-nitrophenyl)acetic acid (HNPAC). X-ray crystallographic data disclosed that Pt(II) center of **NMPt** adopts a square-planar geometry similar to that of nedaplatin. In **NMPt** molecule, the Pt(II) center is coordinated by two oxygen atoms of the hydroxyl and carboxyl groups in HNPAC ligand and two ammine ligands. The quick conversion of **NMPt** (100  $\mu$ M) in PBS buffer upon irradiation at 365 nm was observed, displaying a distinct absorption bathochromic shift from 265 to 300 nm. The  $^1\text{H}$  NMR determination also confirmed the UV irradiation-induced conversion of **NMPt** complex. The CD spectroscopic determination revealed that **NMPt** is able to distort the conformation of CT-DNA only upon UV-irradiation. In addition, agarose gel analysis of plasmid pBR 322 DNA demonstrated that **NMPt** induces plasmid DNA nicking upon UV-irradiation with a distinct dose- and time-dependence. Preliminary results showed that the cytotoxicity of **NMPt** at lower concentration (5–20  $\mu$ M) against human breast adenocarcinoma (MCF-7) cells is comparable to that of nedaplatin upon UV irradiation, while its cytotoxicity is very low without UV irradiation. Therefore, UV irradiation-induced DNA distortion and damage might be correlated to the photo-induced cytotoxicity enhancement for **NMPt**. This study provides an interesting approach for the exploration of photoactivatable Pt(II) complex as anticancer agent, although the photo-induced anticancer activity of **NMPt** remains to be improved.

© 2012 Elsevier B.V. All rights reserved.

### 1. Introduction

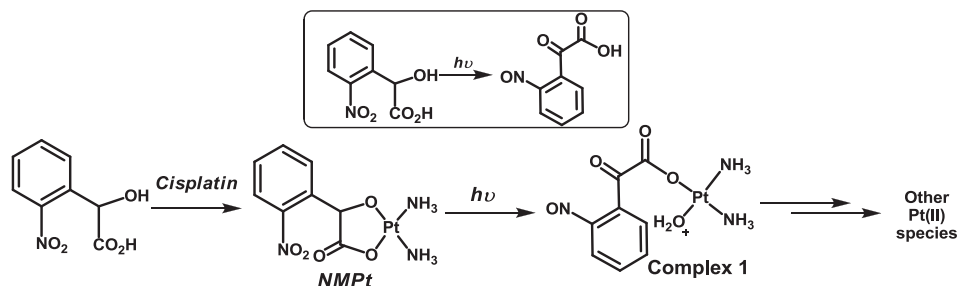
Platinum-based anticancer drugs, including cisplatin, carboplatin, nedaplatin and oxaliplatin have been widely used in clinical treatment of different cancers. However, their clinical application is limited due to their low specificity for tumor tissue, distinct resistance and high toxicity [1]. Various strategies to improve the anticancer behavior of platinum complexes have been adopted. Pt(II) complexes of novel structures such as monofunctional compounds, multinuclear compounds, have been developed to improve their activity and anticancer spectrum [2]. In addition, hybrid anticancer compounds has also been investigated via integrating Pt(II) complex with other anticancer agents such as photodynamic therapy agent [3]. To decrease the side effects of Pt-based anticancer agents, approaches for targeting delivery systems have been explored [4], except for common strategies of integrating targeting groups for tumor with Pt complexes [5]. On the other hand, activating platinum-based prodrugs at specific sites is an attractive alternative to reduce the side effects of these compounds. Pt(IV)

complexes are the most studied prodrugs due to their more inert kinetics than Pt(II) complexes, and their intracellular activation via reduction to Pt(II) species by biological reducing agents should be helpful to overcome certain disadvantages of Pt(II)-based clinical drugs [6]. The tumor-targeting property of Pt(IV) complexes has been demonstrated by Saldler and co-workers, i.e. active Pt(II) species were released by photoactivation of non-toxic diazo Pt(IV) complexes of octahedral geometry [7]. This approach displays a site-specificity for photoactivation, which inspires scientists to develop novel Pt-based complexes for the practical tumor-targeting treatment, and photosensitive Pt(II) complex has also been investigated [8].

Herein, a new photosensitive Pt(II) complex, **NMPt**, was constructed to investigate its anticancer activity especially upon photo-irradiation (Scheme 1). In this complex, the ligand, 2-hydroxy-2-(2-nitrophenyl)acetic acid (HNPAC) is a derivative of photosensitive *o*-nitrobenzyl alcohol. Both of its hydroxyl group and carboxylic anion coordinate to the same Pt(II) center with a chelating effect similar to that of nedaplatin. As the normal *o*-nitrobenzyl alcohol, the photo-induced internal redox process will reduce its nitro group to nitroso group, and the hydroxyl group is oxidized to carbonyl group in the mean time [9]. In fact, this photosensitivity has been frequently utilized to form photo-caged molecules in

\* Corresponding authors. Tel.: +86 25 83597066; fax: +86 25 83314502.

E-mail addresses: [hewej69@nju.edu.cn](mailto:hewej69@nju.edu.cn) (W. He), [zguo@nju.edu.cn](mailto:zguo@nju.edu.cn) (Z. Guo).



**Scheme 1.** Photo-induced conversion of *o*-nitrobenzyl alcohol and the proposed photo-induced conversion of **NMPt** complex.

biological studies [10]. Therefore, the Pt(II) chelating effect of ligand should be decreased distinctly, which may result in a more hydrolytical Pt(II) species, altering its anticancer behavior upon photo-irradiation.

## 2. Results and discussion

### 2.1. Synthesis and characterization of **NMPt**

Ligand HNPAC was prepared from *o*-nitrophenylaldehyde via a two step procedure reported by Rossi and Kao [11]. Then, complex **NMPt** was prepared as a pale yellow powder using a modified procedure for nedaplatin preparation reported by Wang and co-workers [12]. In the MS spectrum of **NMPt**, three signals of  $m/z$  446.92, 870.67 and 1295.17 were observed. These signals can be assigned to  $[M+Na]^+$ ,  $[2M+Na]^+$  and  $[3M+Na]^+$ , respectively by comparing the determined isotopic distribution patterns with the calculated ones given by ISOPRO 3.0 ( $M = \text{NMPt}$ , Fig. 1). This result suggests this complex was stable in the condition of MS determination. Single crystals suitable for X-ray crystallographic determination was obtained by recrystallizing **NMPt** from methanol in fridge at 4 °C. Structural resolution disclosed that this complex crystallizes in

the monoclinic space group of  $P21/c$  (Fig. 2), and there are only one complex molecule and one water molecule in the unit cell. The Pt center was coordinated in a square-planar geometry by two amine nitrogen atoms and two oxygen atoms from hydroxyl and carboxyl groups of HNPAC ligand. With the similar structure to that of nedaplatin, the related coordination bonds around Pt(II) center are almost the same to those found in nedaplatin. For example, the length of Pt1–N1 bond is 2.05 Å, which is almost identical to 2.04 Å found in nedaplatin [13]. Detailed structure parameters have been shown in Table 1. Each water molecule form two hydrogen bonds (Ow–H...O) with two carboxylic O atoms from two different **NMPt** molecules, in addition, this water molecule still form the third hydrogen bond (Ow...H–N) with  $\text{NH}_3$  from the third **NMPt** molecule.

### 2.2. Photolysis of **NMPt**

Although the photosensitivity of *o*-nitrobenzyl derivatives has been reported [9,10], the photosensitivity of **NMPt** formed by HNPAC should be determined. Since **NMPt** has fine aqueous solubility, and the UV–Vis spectrum of **NMPt** was investigated in PBS buffer (100  $\mu\text{M}$ ) of pH 7.4 upon UV irradiation (365 nm) in a photoreactor. **NMPt** displays a stable absorption spectrum without UV irradiation, showing a minor band centered at 262 nm with an extinction coefficient of 4217.9  $\text{M}^{-1}\text{cm}^{-1}$ . Upon UV irradiation, the UV–Vis spectra of **NMPt** were recorded every 20 s, and a new absorption band centered at 300 nm was observed upon UV irradiation. This band increased gradually with the irradiation time accompanied by a gradual decrease of former band at 262 nm (Fig. 3), implying there is a photo-induced conversion of **NMPt** complex. The UV–Vis spectra became stable in 3 min, displaying the photo-induced conversion has been finished, and the final extinction coefficient at 300 nm is 5203.4  $\text{M}^{-1}\text{cm}^{-1}$ . The clear isobestic points at 255 and 276 nm also confirmed the conversion process, and the solution of **NMPt** turned from colorless to pale brown. Since the absorbance at 300 nm is the characteristic band of *o*-nitrosophenyl group, a typical change of *o*-nitrobenzyl alcohol derivatives to *o*-nitrosophenyl group upon UV irradiation should

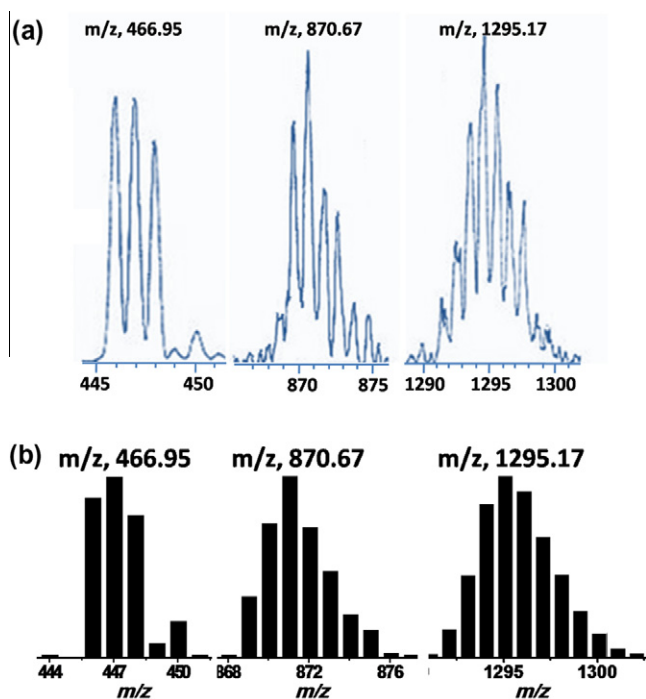


**Fig. 1.** (A) Observed isotopic distribution patterns (IDPs) of main signals found in the ESI-MS spectrum of complex **NMPt**. (B) Calculated IDPs of  $[\text{NMPt} + \text{Na}]^+$ ,  $[2\text{NMPt} + \text{Na}]^+$ , and  $[3\text{NMPt} + \text{Na}]^+$ .

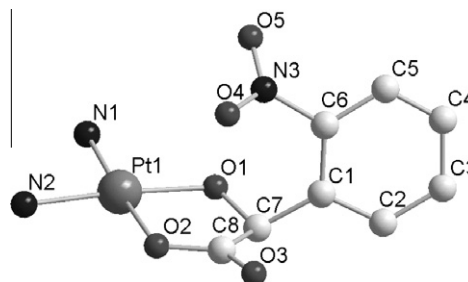


**Fig. 2.** Molecular structure of **NMPt**. Water molecule and hydrogen atoms were omitted for clarity.

**Table 1**  
Selected bond lengths (Å) and angles (°) for **NMPt**.

Pt(1)–N(1)	2.045(7)	O(1)–Pt(1)–N(1)	92.9(3)
Pt(1)–N(2)	2.030(8)	O(1)–Pt(1)–O(2)	85.1(3)
Pt(1)–O(1)	2.005(6)	N(2)–Pt(1)–O(2)	91.7(3)
Pt(1)–O(2)	2.054(7)	N(2)–Pt(1)–N(1)	90.5(3)
		N(1)–Pt(1)–O(2)	176.7(2)

be occurred. The bathochromic shift of absorbance from 262 to 300 nm for **NMPt** complex suggested a Norrish type II photoreaction.

The photosensitivity of complex **NMPt** (5 mM) has also been investigated using  $^1\text{H}$  NMR spectroscopy in  $\text{D}_2\text{O}$ . Similar to the UV–Vis determination, stable  $^1\text{H}$  NMR spectrum was observed and new peaks were observed in the down field only upon UV irradiation. As shown in Fig. 4, the three new minor signals labeled with asterisk can be assigned as signals for protons  $b'$ ,  $c'$  and  $d'$ . It is the result of down-field shift of signals for protons  $b$ ,  $c$  and  $d$  due to the photo-induced conversion of **NMPt** to complex **1**. It is clear that the conversion of **NMPt** to complex **1** will decrease the density of delocalized electrons of phenyl ring due to the formation carbonyl group at the para position of nitro group, which caused the down-field shift for the signals of the three protons on aromatic ring. According to the rule to estimate chemical shift of protons on aromatic ring, this Norrish type II conversion of HNPAC would induce a neglectable down-field shift for proton  $a$ , which is consistent with our observed spectra. The  $^1\text{H}$  NMR data implied that only 10% of **NMPt** has been converted into complex **1** in  $\text{D}_2\text{O}$  after 10 min of UV irradiation. Longer photo-irradiation resulted in a distinct brown precipitate.

### 2.3. CD spectra of CT-DNA in the presence of **NMPt**

It was well recognized that the formation of covalent cross links between platinum complex and DNA is closely related to the anticancer activity of platinum-based drugs. Therefore, the DNA binding behavior of **NMPt** was investigated with or without UV irradiation to explore whether photo-irradiation would alter its DNA binding behavior. As shown in Fig. 5, the CD spectra of CT-DNA (0.1 mM) displayed that 40 h of incubation with **NMPt** at 37 °C in dark did not induce any obvious change at all tested [**NMPt**]/[DNA] ratio (0–2.0), implying poor DNA binding ability of **NMPt**. However, if the mixture of CT-DNA and **NMPt** was UV-irradiated for 3 min before incubation, both the negative (245 nm) and positive (275 nm) bands of CD spectrum of CT-DNA decreased in intensity after 40 h of incubation in dark. Higher complex concentration resulted in a larger decrement. It seems that both the DNA

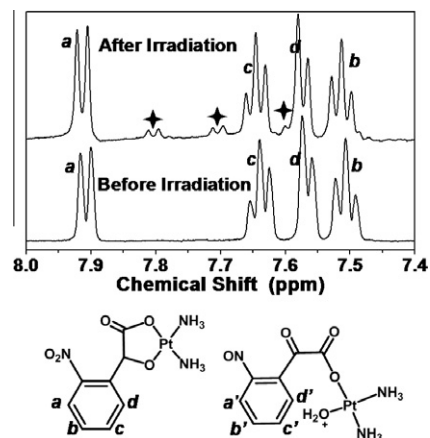


**Fig. 4.**  $^1\text{H}$  NMR spectra of **NMPt** in  $\text{D}_2\text{O}$  determined before and after 10 min of irradiation. The signals labeled with asterisks are the new signals observed after irradiation in the down field.

helicity and base stacking can be altered by the irradiated complex. These results suggested that the photo-irradiation is able to convert **NMPt** of poor DNA binding ability into species which can interact with DNA effectively.

### 2.4. Agarose gel electrophoresis of plasmid pBR322 DNA in the presence of **NMPt**

Agarose gel assay of supercoiled DNA (plasmid pBR322 DNA) mixing with **NMPt** has also been carried out to explore the photo-irradiation effect of **NMPt** on the interaction between plasmid DNA and **NMPt**. Therefore, DNA (200 ng/ $\mu\text{L}$ ) was incubated with **NMPt** (0–100  $\mu\text{M}$ ) at 37 °C with or without UV irradiation for 3 h. As can be seen from Fig. 6, incubating plasmid DNA with **NMPt** (100  $\mu\text{M}$ ) in dark for 3 h resulted in supercoiled DNA (form I) with very minor nicked DNA (Form II, lane 1). Photo-irradiation of DNA with no **NMPt** complex for 3 h displayed a similar gel pattern with only nicked DNA being slightly enhanced (Lane 2). The gel patterns shown in lanes 1 and 2 suggested that either **NMPt** or UV irradiation alone could not disturb supercoiled DNA. Distinct enhancement of nicked DNA was observed only upon UV irradiation in the presence of **NMPt** (Lanes 3–6). The accompanied decrease of form I DNA was also observed in the mean time. Higher **NMPt** concentration resulted in larger amount of nicked DNA and smaller amount of form I DNA. Besides the distinct dose-dependent nicking efficiency of supercoiled DNA promoted by **NMPt**, the cleavage to form nicked DNA can also be promoted by

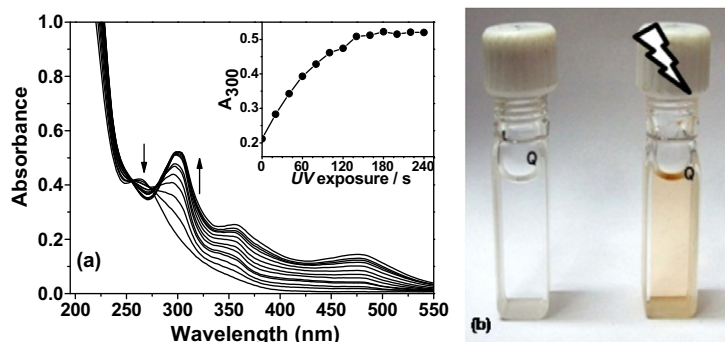


**Fig. 3.** (a) UV–Vis spectra of 100  $\mu\text{M}$  **NMPt** in PBS buffer (100  $\mu\text{M}$ , pH 7.4) determined upon UV irradiation (365 nm, 4 min) in a photoreactor. The spectra were recorded with an interval of 20 s. Inset is the temporal profile of absorbance at 300 nm upon UV-irradiation. (b) Photograph of non-irradiated and UV-irradiated **NMPt** (100  $\mu\text{M}$ ) solutions in PBS buffer.

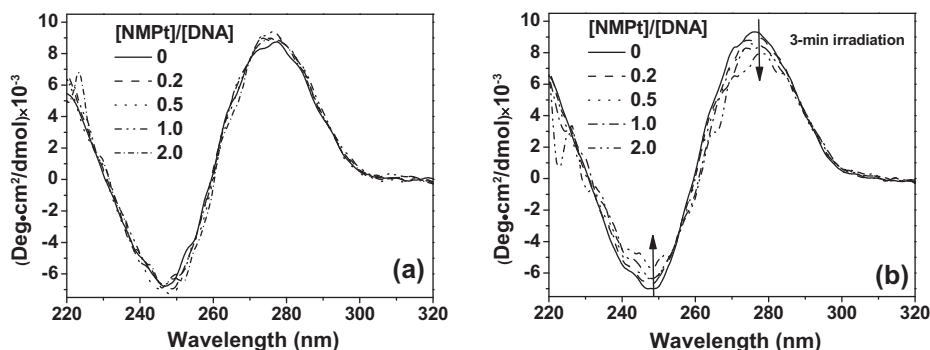


**Fig. 5.** CD spectra of CT-DNA (0.1 mM) treated with complex **NMPt** at different  $[\text{NMPt}]/[\text{DNA}]$  ratios (0–2.0). (a) Spectra determined after 40 h of incubation with **NMPt** at 37 °C in dark; (b) spectra determined after 40 h of incubation with **NMPt** which has been UV-irradiated at 365 nm for 3 min.

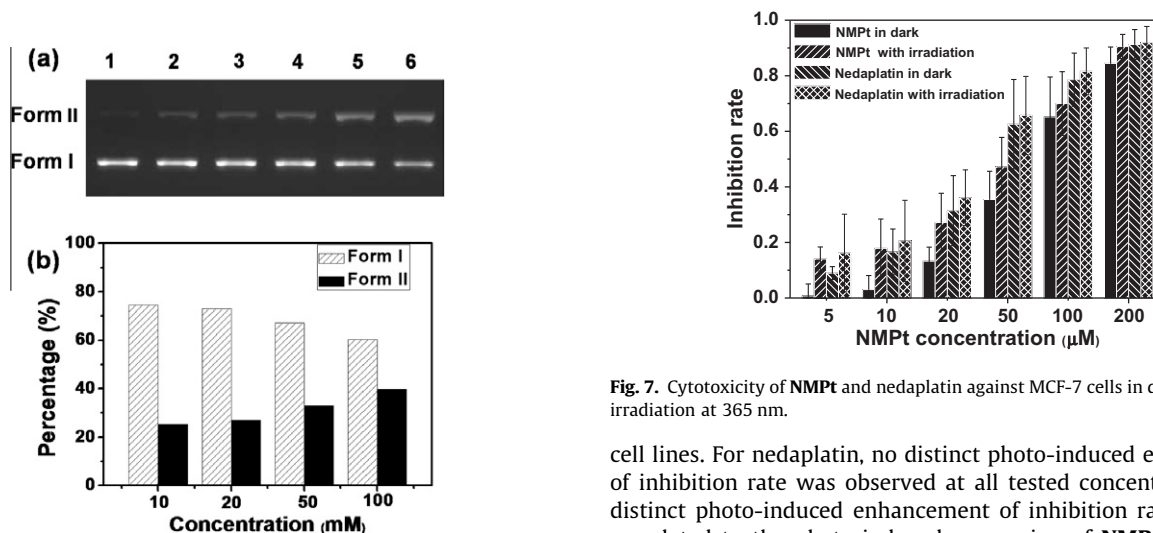


**Fig. 6.** (a) Agarose gel electrophoresis patterns of plasmid pBR322 DNA (200 ng/ $\mu\text{L}$ ) incubated with complex **NMPt** of different concentrations at 37 °C. Concentration of **NMPt** for Lanes 2–6: 0, 10  $\mu\text{M}$ , 20  $\mu\text{M}$ , 50  $\mu\text{M}$ , 100  $\mu\text{M}$ , and the UV-irradiation time is 3 h. Lane 1: control of DNA incubated with 100  $\mu\text{M}$  **NMPt** in dark. (b) The related histogram of percentages of Form I and Form II DNA induced by photo-irradiation in the presence of **NMPt** complex.

increasing the photo-irradiation time at the same **NMPt** concentration. All these results indicated that photo-irradiation is able to induce the cleavage of DNA in the presence of **NMPt**.

### 2.5. Cytotoxicity of **NMPt** against human breast adenocarcinoma cells (MCF-7 cells)

On the basis of the above mentioned experimental results, the cytotoxicity of **NMPt** against human breast adenocarcinoma cells (MCF-7) was determined respectively with or without UV irradiation. Nedaplatin was taken as a positive control for comparison due to their similar coordination structure. For **NMPt**, the distinct photo-induced enhancement of inhibition rate was observed when the incubation concentration is lower (Fig. 7). For example, **NMPt** showed almost no inhibition to MCF-7 cells at 5  $\mu\text{M}$ , while  $\sim 13\%$  inhibition rate was observed upon photo-irradiation. The inhibition rate in dark is  $\sim 3\%$  at 10  $\mu\text{M}$  of **NMPt**, while it was enhanced to  $\sim 18\%$  upon photo-irradiation. The photo-irradiation induced enhancement factor for **NMPt** is above 6-fold at these two cases. Interestingly, when the **NMPt** concentration was increased from 20 to 200  $\mu\text{M}$ , the irradiation-induced enhancement factor for inhibition rate was reduced quickly, and the photo-induced enhancement factor at 100  $\mu\text{M}$  is  $\sim 1.1$ -fold. This demands more detailed biological investigation and further experiments on other

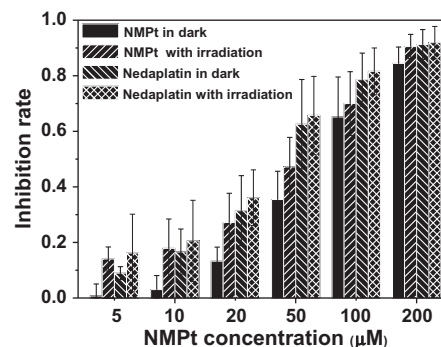


**Fig. 7.** Cytotoxicity of **NMPt** and nedaplatin against MCF-7 cells in dark or upon UV irradiation at 365 nm.

cell lines. For nedaplatin, no distinct photo-induced enhancement of inhibition rate was observed at all tested concentrations. The distinct photo-induced enhancement of inhibition rate might be correlated to the photo-induced conversion of **NMPt**, which enhances the DNA binding ability and alters DNA conformation. In addition, the photo-induced DNA nuclease activity may also contribute to the photo-induced enhancement of anticancer activity at lower concentration. It should be noted that **NMPt** displayed a very lower cytotoxicity to MCF-7 cells at lower complex concentration ( $\leq 10 \mu\text{M}$ ) in dark, when compared with nedaplatin. However, photo-irradiation enhanced its cytotoxicity to be comparable to that of nedaplatin at same concentration without UV irradiation.

### 3. Conclusion

A new photo-sensitive complex, **NMPt**, was prepared with a photo-sensitive *o*-nitrobenzyl derivative as ligand. This complex possesses a similar structure to that of nedaplatin, and displays a distinct photo-induced conversion upon UV irradiation. Enhanced DNA binding and cleavage activities were also observed upon UV irradiation. Although the inhibition rate of **NMPt** to MCF-7 cells is low in dark at lower concentration, photo-irradiation promotes its cytotoxicity to a level comparable to that of nedaplatin in dark at the same concentration. Further biological investigations are warranted to reveal the molecular mechanism of **NMPt**, which will provides helpful insights into the rational design of photoactivatable platinum-based antitumor complexes.

### 4. Experimental

#### 4.1. Material and methods

All chemicals and solvents were of reagent grade and used as received.  $^1\text{H}$  NMR spectra were recorded on a Bruker DRX-500

spectrometer. Electrospray mass spectra were determined using an LCQ electron spray mass spectrometer (ESI-MS, Finnigan). The isotopic distribution patterns for the complex were simulated by ISOPRO 3.0 program. UV–Vis spectra were recorded with a UV-2550 photospectrometer (Shimadzu). X-ray crystallographic data were recorded on a Siemens Bruker SMART CCD diffractometer using graphite monochromatized Mo K $\alpha$  radiation ( $\lambda = 0.71037 \text{ \AA}$ ). The crystal structure was resolved by direct methods using the program SHELXL-97 [12]. Photolysis experiments were all performed in photoreactor offered by Xujiang company, Nanjing.

#### 4.2. Preparation of **NMPt**

Ligand HNPAC was synthesized according to the reported procedure [11]. **NMPt** were synthesized in dark using a modified procedure for nedaplatin [12]. Therefore, cisplatin (600 mg) were suspended in 25 mL water and 624 mg Ag<sub>2</sub>SO<sub>4</sub> were added with stirring. After being stirred at room temperature for 24 h, the precipitates were removed by filtration. The obtained filtrate was mixed with a methanolic solution (20 mL) containing 375 mg HNPAC. Then, an aqueous solution prepared by dissolving 599 mg Ba(OH)<sub>2</sub>·8H<sub>2</sub>O in 20 mL water was added dropwise into the mixture in 6 h with stirring. After stirring in dark at room temperature for 48 h, the precipitate was removed by filtration and 50 mL methanol was added. Then, the solvents were removed in vacuo and the residue was washed by methanol and acetone in sequence. **NMPt** (310 mg) was obtained as pale yellow powders with a yield of 38%. The single crystal for crystal structure resolution was obtained by slow evaporation of its methanolic solution. <sup>1</sup>H NMR (500 MHz, DMSO-*d*<sup>6</sup>,  $\delta$ , ppm): 8.14 (d, *J* = 7.6 Hz, 1H), 7.71 (d, *J* = 8.0 Hz, 1H), 7.62 (t, *J* = 7.3 Hz, 1H), 7.41 (t, *J* = 7.7 Hz, 1H), 5.55 (s, 1H). ESI-MS (*m/z*, positive mode): found 446.9, calcd. 447.0 for [M+Na]<sup>+</sup>; found 870.7, calcd. 871.1 [2M+Na]<sup>+</sup>; found 1294.7, calcd. 1295.1 for [3M+Na]<sup>+</sup>.

#### 4.3. UV–Vis and <sup>1</sup>H NMR spectra of **NMPt** upon UV irradiation

One hundred micromolar of **NMPt** in PBS buffer (100  $\mu$ M, pH 7.4) were added into a cylindrical quartz cuvette and irradiated in a photoreactor equipped with a filter of 365 nm, and UV–Vis spectra were recorded every 20 s until no change was observed.

In addition, <sup>1</sup>H NMR spectra of **NMPt** in D<sub>2</sub>O (5 mM) were determined also before and after UV irradiation for 10 min.

#### 4.4. CD spectra of CT-DNA in the presence of **NMPt** upon UV irradiation

CD spectra of CT-DNA in Tris–HCl buffer (5 mM Tris–HCl, 50 mM NaCl, pH 7.4) in the absence or presence of **NMPt** were determined, respectively at the [NMPt]/[DNA] ratio of 0, 0.2, 0.5, 1.0, 2.0. Therefore, two groups of samples, non-irradiated and UV-irradiated ones were investigated, respectively. For the irradiated group, all the samples were irradiated for 3 min in a photoreactor with a filter of 365 nm. Then, the samples were incubated at 37 °C for 40 h before recording CD spectra. For the non-irradiated group, all the samples were directly incubated at 37 °C for 40 h before measurement. All the CD spectra were recorded with Tris–HCl buffer as reference using a scanning rate of 20 nm/min in the range of 220–320 nm.

#### 4.5. Photo-induced nuclease activity of **NMPt**

To investigate the photo-induced nuclease activity of **NMPt**, 500 ng/ $\mu$ L plasmid pBR322 DNA were mixed with different amount of complex **NMPt** in Tris–HCl buffer, and the final DNA concentration in all samples was adjusted to be 200 ng/ $\mu$ L with a total volume of 10  $\mu$ L. All samples with **NMPt** were incubated at 37 °C upon

irradiation in photoreactor with a filter of 365 nm. The DNA without **NMPt** was irradiated and incubated as control. In addition, DNA incubated **NMPt** (100  $\mu$ M) incubated at 37 °C without irradiation was also measured as a control. After being mixed with 2  $\mu$ L loading buffer, all the quenched samples were loaded respectively onto a 1% agarose gel. Electrophoresis was carried out in TAE buffer (40 mM Tris–acetate/1 mM EDTA) at 60 V for 2–3 h. Gels were stained with ethidium bromide and visualized using UVP gel doc system, and the gel patterns were analyzed with Quantity One 4.6.2.

#### 4.6. Cytotoxicity of **NMPt** against MCF-7 cells

Cytotoxicity of **NMPt** against MCF-7 cell lines were tested by MTT assay. MCF-7 cells were seeded in a 96-well plate and incubated in Dulbecco's modified Eagle medium (DMEM) overnight. **NMPt** in PBS buffer solution (pH 7.4) were added to the culture medium to a desired concentration. The irradiation was carried out by UV irradiation at 365 nm for 3 min. Then the cells were incubated for 48 h and 20  $\mu$ L MTT (5 mg/mL) were added to the wells, respectively. The medium were removed after 4 h of incubation. Then, 200  $\mu$ L DMSO were added to each well and the absorbance was measured at 570 nm using plate reader (Varioskan Flash, Thermo Scientific). Each assay was performed independently three times. The inhibition rate was assessed using the following equation:

$$\% \text{Inhibition rate} = (\text{OD}_{\text{control}} - \text{OD}_{\text{drug}}) / (\text{OD}_{\text{control}} - \text{OD}_{\text{blank}}) \times 100$$

#### Acknowledgments

We thank the National Basic Research Program of China (No. 2011CB935800) and National Natural Science Foundation of China (No. 10979019, 21131003, 90713001 and 21021062) for financial support.

#### Appendix A. Supplementary material

Supplementary data associated with this article can be found, in the online version, at <http://dx.doi.org/10.1016/j.ica.2012.06.047>.

#### References

- [1] X. Wang, Z. Guo, *Bioinorganic Medicinal Chemistry*, Wiley-VCH Verlag GmbH & Co. KGaA, 2011. pp. 97–149.
- [2] (a) K.S. Lovejoy, R.C. Todd, S. Zhang, M.S. McCormick, J.A. D'Aquino, J.T. Reardon, A. Sancar, K.M. Giacomini, S.J. Lippard, *Proc. Natl. Acad. Sci. USA* 105 (2008) 8902; (b) Y. Zhao, W. He, P. Shi, J. Zhu, L. Qiu, L. Lin, Z. Guo, *Dalton Trans.* (2006) 2617; (c) J. Zhang, X. Wang, C. Tu, J. Lin, J. Ding, L. Lin, Z. Wang, C. He, C. Yan, X. You, Z. Guo, *J. Med. Chem.* 46 (2003) 3502; (d) Farrell, in: J.H. Hurley, J.B. Chaires (Eds.), *Advances in DNA Sequence Specific Agents*, vol. 2, JAI Press Inc., Greenwich, CT, 1996, p. 187; (e) J.W. Cox, S.J. Berners-Price, M.S. Davies, W. Barklage, Y. Qu, N. Farrell, *J. Am. Chem. Soc.* 123 (2001) 1316.
- [3] J. Mao, Y. Zhang, J. Zhu, C. Zhang, Z. Guo, *Chem. Commun.* (2009) 908.
- [4] (a) Z. Yang, X. Wang, H. Diao, J. Zhang, H. Li, H. Sun, Z. Guo, *Chem. Commun.* (2007) 3453; (b) J.A. MacDiarmid, N.B. Mugridge, J.C. Weiss, L. Phillips, A.L. Burn, R.P. Paulin, J.E. Haasdyk, K.-A. Dickson, V.N. Brahmabhatt, S.T. Pattison, A.C. James, G.A. Bakri, R.C. Straw, B. Stillman, R.M. Graham, H. Brahmabhatt, *Cancer Cell* 11 (2007) 431.
- [5] (a) K.R. Barnes, A. Kutikov, S.J. Lippard, *Chem. Biol.* 11 (2004) 557; (b) W.H. Ang, I. Khalaila, C.S. Allardyce, L. Juillerat-Jeanneret, P.J. Dyson, *J. Am. Chem. Soc.* 127 (2005) 1382; (c) R.P. Feazell, N. Nakayama-Ratchford, H. Dai, S.J. Lippard, *J. Am. Chem. Soc.* 129 (2007) 8438.
- [6] M.D. Hall, H.R. Mellor, R. Callaghan, T.W. Hambley, *J. Med. Chem.* 50 (2007) 3403.
- [7] (a) P.J. Bednarski, R. Grunert, M. Zielzki, A. Wellner, F.S. Mackay, P.J. Sadler, *Chem. Biol.* 13 (2006) 61; (b) F.S. Mackay, J.A. Woods, H. Moseley, J. Ferguson, A. Dawson, S. Parsons, P.J. Sadler, *Chem. Eur. J.* 12 (2006) 3155.

- [8] K.L. Ciesinski, L.M. Hyman, D.T. Yang, K.L. Haas, M.G. Dickens, R.J. Holbrook, K.J. Franz, *Eur. J. Inorg. Chem.* (2010) 2224.
- [9] (a) G.C.R. Ellis-Davies, *Chem. Rev.* 108 (2008) 1603;  
(b) R. Reinhard, B.F. Schmidt, *J. Org. Chem.* 63 (1998) 2434.
- [10] A. Deiters, *ChemBioChem* 11 (2009) 47.
- [11] F.M. Rossi, J.P.Y. Kao, *J. Biol. Chem.* 272 (1997) 3266.
- [12] Z. Meng, Y. Zhao, L. Tang, H. Wang, *Chin. J. Pharm.* 34 (2003) 268.
- [13] Q.K. Wang, S.P. Pu, Y.W. Cong, Y.N. Li, C.F. Luan, *Acta Crystallogr., Sect. E: Struct. Rep. Online* 65 (2009) m1687.